K. A. Alipbayev[1] [1], *Associate Professor*, PhD, **K. S. Saurova**[2] [2], *Senior lecturer*, **G. Daukeev**[3]

METHOD OF INCREASING THE ACCURACY OF THE STAR SENSOR

Ua   Розглядаються новий алгоритм фільтрації спотворень глибокого зображення зоряного неба для підвищення точності визначення положення зірки - виявлення центроїда. Досліджується підвищення точності виміру параметрів орієнтації космічного апарату зірковими датчиками. Застосований метод обчислень, що використовує алгоритм точної оцінки центроїду, що відновлює функцію розкидання точок за астрономічними зображеннями. Запропоновано мінімізацію ефектів турбулентності атмосфери та шумів системи на зображеннях із тривалою експозицією, отриманих наземним телескопом. Метод перевірено у середовищі MATLAB для реального зображення глибокого неба, записаного наземною системою.

En   A new algorithm for filtering distortions of the deep image of the starry sky is considered to improve the accuracy of determining the position of the star - the detection of the centroid. An increase in the accuracy of measuring the orientation parameters of the spacecraft by stellar sensors is being investigated. The method of calculations using the algorithm of exact estimation of the centroid is applied, restoring the function of the scatter of points from recorded astronomical images. Minimization of the effects of atmospheric turbulence and system noise on long-exposure images obtained by a ground-based telescope is proposed. The method was tested in the MATLAB environment for a real image of the deep sky recorded by the ground system.

Introduction

The star sensor (SS) is capable of determining the orientation parameters of the spacecraft with high accuracy, but under favorable light conditions and in a limited range of its angular velocities [1].

Many works have been devoted to the study of SS errors. In [2], errors are considered based on flight experiment data. The errors caused by thermoelastic deformations are investigated [3], the issues of electromagnetic compatibility are considered [4], the use of SS to identify the parameters of the error model of the inertial navigation system of the upper stage [5] etc. The influence of SS errors

---

[1] *Almaty University of Energy and Communications*
[2] *Almaty University of Energy and Communications*
[3] *Almaty University of Energy and Communications*

on the accuracy of spacecraft orientation systems and platform stabilization are considered in [6 – 9].

The main issues and stages of CAD of the optical SS system are considered [10], the results of testing software and mathematical support [11], the influence of the methodological error of the SS on the accuracy of processing and determination of orientation by stars [12].

However, the issue of improving the accuracy of the SS by eliminating or compensating for interference arising in it remains relevant.

Problem statement

The purpose of the article is to develop a method and algorithm for filtering distortions of the deep image of the starry sky to improve the accuracy of determining the position of a star, that is, detecting a centroid.

The main content

We apply the Quaternion Estimation (QUEST) method to determine the spatial angular position of a nanosatellite. To do this, it is necessary to implement an algorithm for searching for the centroids of stars visible in the image; a geometric voting algorithm for identifying star images. To evaluate the operability of algorithms (sky coverage, memory requirements, computing time, etc.), we will simulate algorithms for idealized and real input parameters using a specially developed software package for testing.

To identify the area of the starry sky, the entire area of the image is scanned with the search for pixels with brightness higher than a predefined threshold value, which is determined during calibration and construction of the image of the real sky.

When identifying a pixel with a brightness exceeding the set threshold, the process of area growth is started, during which the number of pixels in the area is counted. At this stage, hot pixels are filtered – cosmic ray hits and extended objects. At the end of the image plane search, all areas corresponding to the stars are identified with the assignment of an identification number. They define the centroid of each area with coordinates

$$x = \frac{\sum_{i=1}^{n} x_i \cdot I_i}{\sum_{i=1}^{n} I_i}, \quad = \frac{\sum_{i=1}^{n} y_i \cdot I_i}{\sum_{i=1}^{n} I_i}, \tag{1}$$

where (x_i, y_i) are the (x, y) coordinates of the i-th pixel in the area, I_i – is the intensity of the i-th pixel in the area. The coordinates are described in the coordinate system of the image plane.

To identify the stars, a geometric voting algorithm was used, in which the angles between each pair of stars detected in the image are compared with the angles between pairs of stars in the star catalog. The positions of the stars in the

coordinate system of the image plane are converted into unit vectors in the coordinate system of the sensor.

The vecto $\vec{\vartheta}$, to be rotated is given by the values of its projections on the axis of the original coordinate system:

$$
\vec{\vartheta} = \begin{bmatrix} u_x \\ u_y \\ u_z \end{bmatrix} = \left(1 + \left((x_u - x_c)\frac{pp_x}{f_m m} \right)^2 + \left((y_u - y_c)\frac{pp_y}{f_m m} \right)^2 \right)^{(-1/2)} \times
$$

$$
\times \begin{bmatrix} (x_u - x_c)\dfrac{pp_x}{f_{mm}} \\ (y_u - y_c)\dfrac{pp_y}{f_{mm}} \\ 1 \end{bmatrix} , \tag{2}
$$

where (u_x, u_y, u_z) are the components of the star vector in the sensor coordinate system, (x_u, y_u) are the coordinates of the centroids in the coordinate system of the image plane, (x_c, y_c) are the coordinates of the main point (the point at which the optical axis intersects the detector) in the coordinate system of the image plane, (pp_x, pp_y) – pixel sizes in the x and y directions of the image sensor, respectively, f_{mm} – is the focal length of the image. The angle between each pair of depicted stars is obtained by the scalar product of their unit vectors.

To calculate the rotation quaternion between the Earth-Centered inertial (ECI) coordinate systems and the sensor $\upsilon_{kb} = R_{bi}\upsilon_{ki}$ the QUEST algorithm is used. At the same time, the loss function is minimized

$$
J(R_{bi}) = \frac{1}{2}\sum_{k=1}^{n}\omega_k \left| v_{kb} - R_{bi}v_{ki} \right|^2 , \tag{3}
$$

where ω_k – a set of weights assigned to each dimension of a pair of vectors: unit vectors in v_{ki} the ECI coordinate system and v_{kb} in the coordinate system of the sensor housing. The matrix R_{bi} it is identified by a statistical method in which a set of measurements v_{kb} identified by the geometric voting algorithm by v_{ki} .

Minimization of J can be solved by finding the largest eigenvalue of the R_{bi} matrix. However, this involves a significant amount of computation. To get around this problem, an approximation of this process has been developed. The image is modeled by generating a Gaussian distribution of the Point Spread Function (PSF) system with a full width at half height (FWHM) equal to 4 pixels. This image is created by a two-dimensional function for an array of 1024×1024 pixels, x and y changes as 1, 2, ..., 1024

$$G(x, y) = \frac{1}{\sigma\sqrt{2\pi}} exp^{-\frac{(x-x_c)^2 + (y-y_c)^2}{2\sigma^2}} \tag{4}$$

$$\sigma = \frac{FWHM}{2\sqrt{2\log 2}} \ , \tag{5}$$

where (x_c, y_c) is the coordinate of the ideal center of the star in the image plane; σ is the variance of the Gaussian function;

To reduce the search time of the image plane, only each alternative pixel is found. Sampling at every 4th pixel speeds up the process even more, but there is a chance of missing a real star, because by default FWHM = 4. The time allotted for each search method is shown in Table 1.

Table **1.**

Image plane search time

Pixel increment	Number of pixels checked	Time required
1 pixel	1048576	0,0955 sec
2 pixel	262144	0,0293 sec
3 pixel	65536	0,0102 sec

Since the exposure time of the image is always the same, it is possible to estimate the noise introduced by the reading mechanism, dark noise and fixed structural noise. Knowing these characteristics and assuming a different signal-to-noise ratio (SNR) for the image of the star, the corresponding Gaussian noise is added to the image of the star. The average value of Gaussian noise is the dark value, and its standard deviation is the sum of the read and dark noise.

Thus, the implementation of the complete centroid algorithm represents a sequence including the image plane, search, build-up, region segmentation and centroid. This is done on a reference image, where, unlike the ideal case, the calculated centroid has positional uncertainty (added noise). The simulation is repeated on 1000 images with randomly changing coordinates of the centroid of the star, and the displacement of the centroid is recorded on each image. The standard deviation of these 1000 values gives the uncertainty introduced by the centroid algorithm. This uncertainty depends on the signal-to-noise ratio (Table 2).

Table **2.**

Signal/noise

SNR	Gentroiding error (arcsec)
30	8,42
15	6,82
10	8,86

SNR	Gentroiding error (arcsec)
5	6,6
4.5	7,3
3.5	8,33
3.3	11,96
3.2	13,47
3.1	17,37
3	27,46

The simulation performed with different signal-to-noise ratios assumes that not a single star with an SNR> 3 σ is missed when using alternative pixel scanning. The SNR is set by changing the noise level and keeping the brightness of the star constant. The PSF method is more accurate, especially at high SNR.

According to these stars, a catalog table of pairs of angles according to the catalog is formed. The sky with different limiting stellar magnitudes has a different number of entries in the catalog table of a pair of angles, depending on the number of stars in the sky. The size of this directory is taken into account when choosing the size of the flash memory (Table 3).

Table **3.**

Pairs of corners by catalog

Limiting Magnitude	No. of stars	No. of entries
5,0	1608	11671
5,5	2819	35493
6,0	4995	108656
6,5	8789	332092

To evaluate the performance of the QUEST algorithm, we will model the ideal input data in a similar way to the geometric voting algorithm. According to the known unit vectors of stars in the ECI coordinate system, visible in each field from the list of unit vectors of the star catalog, their unit vectors in the sensor coordinate system are modeled. To do this, the matrix of transition (rotation) from the ECI to the coordinate system of the sensor housing for the selected field is used

$$R_{bi} = \begin{bmatrix} \cos\alpha \cos\delta & -\cos\alpha \sin\delta & \sin\alpha \\ \sin\delta & \cos\delta & 0 \\ -\sin\alpha \cos\delta & \sin\alpha \sin\delta & \cos\alpha \end{bmatrix}, \qquad (6)$$

where α and δ are the right ascension and declination of the center of the camera's field of view. The unit vectors in the coordinate system of the sensor of stars visible in this field are the product of the rotation matrix by their unit of measurement. Then from R_{bi} the ideal quaternion will be

$$q_{ideal} = \begin{bmatrix} q_1 \\ q_2 \\ q_3 \end{bmatrix} = \begin{bmatrix} \dfrac{m_{21} - m_{12}}{2\sqrt{1 + m_{00} + m_{11} + m_{22}}} \\ \dfrac{m_{02} - m_{20}}{2\sqrt{1 + m_{00} + m_{11} + m_{22}}} \\ \dfrac{m_{10} - m_{01}}{2\sqrt{1 + m_{00} + m_{11} + m_{22}}} \end{bmatrix}, \tag{7}$$

where m_{00}, m_{01}, m_{02}, m_{10}, …, m_{20} are the elements of the rotation matrix. The output quaternion is compared with the quaternion (7) by calculating the distance between these quaternions using their scalar product

$$d = \cos^{-1}(2q_{ideal} \cdot q_{quest} - 1). \ d \tag{8}$$

To calculate quaternions, the criterion of having at least 5 stars in any given field is selected. Hence, the number of fields in the sky with more than 5 stars in the field determines the sky coverage for the QUEST algorithm. The quaternion distance is calculated for all fields in the sky. Its standard deviation (RMS error) gives the accuracy of the QUEST algorithm. The number of fields in the sky with more than 5 stars in the field and the accuracy of the QUEST algorithm are shown in Table 4.

Table **4.**

QUEST execution for different limit values

Limiting Magnitude	Sky Coverage	RMS error (deg)
5,0	52,66%	$6,866 \cdot 10^{-7}$
5,5	83,16%	$7,00 \ \cdot 10^{-7}$
6,0	98,61%	$6,929 \ \cdot 10^{-7}$
6,5	100%	$7,12 \ \cdot 10^{-7}$

The algorithm for identifying stars is based on a geometric voting scheme in which a pair of stars in the catalog votes for a pair of stars in the image if the angular distance between the stars of both pairs is the same. Once the identity of the stars is determined, the camera position is calculated by the quaternion method. Figure 1 shows part of the sky map around the star S.
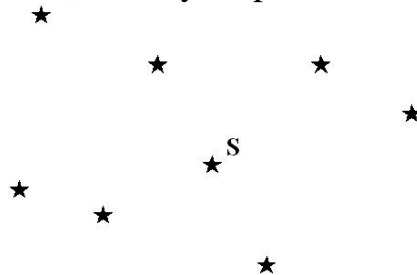

Fig. 1. Example of a star pattern

Each star in the catalog is associated with a sparse matrix in which zeros are in empty cells and ones are in cells with stars.

The comparison is performed by comparing the information of the star catalog with the stars found in the image. Despite the fact that the catalog includes information about intensity, as well as information about location, brightness is used only as a secondary, additional filter.

The algorithm consists of five modules:

– Image simulation. The user can specify the internal parameters of the camera and its position, and the system filters the image taken by the camera, taking into account these parameters. It can filter the sequence of images when speed orientation parameters are also set.

– Lost in space. This module runs the Laboratory Information System (LIS) algorithm both on reference and on real images. Its input data is a star catalog and either internal and external camera parameters or an image. Its result is an estimated rotation matrix and observed stellar identifiers.

– Tracking. The tracking process can be performed in real time on a sequence of reference or real images.

– Image capture. Images are captured from a camera connected to a computer and sent to the LIS, or tracking module.

– Calibration. In addition to the standard calibration procedure, this module calibrates cameras using star images.

In the presence of a priori sensor motion data obtained from third-party devices, or pre-calculated using LIS algorithms, the position of stars in the detector system can be predicted with high accuracy. In this case, the tasks of recognition and determination are reduced to the task of maintenance performed according to the forecast-correction scheme, which significantly increases the performance of the system as a whole.

The accuracy of the centroid affects both LIS and tracking performance. The probability of correct identification of the star depends on this accuracy, as well as the overall accuracy of the star tracker. Star detection and centroid estimation are the first steps of the algorithms.

The result of the study of two methods for estimating the centroid: the simple center of mass method, and the PSF table method based on comparing the normalized pixel values of the image with the theoretical pixel values that would be obtained using a silent PSF are shown in fig. 2.

The probability of correct recognition of stars is significantly affected by errors in estimating the brightness of stars when using algorithms based on brightness [13]. Since the catalog stores the visual magnitude, while the brightness of the image stars depends on the magnitude, it is impossible to predict the brightness of the image stars from the brightness of the catalog stars. In addition, brightness values are more sensitive to noise and camera malfunctions.

We use the method of calculating the centroid by an algorithm for accurate estimation of the centroid, which restores the point spread function (PSF)

from recorded astronomical images. The results for three different stars S1, S2, S3 and the reference calculation are shown in fig. 3.
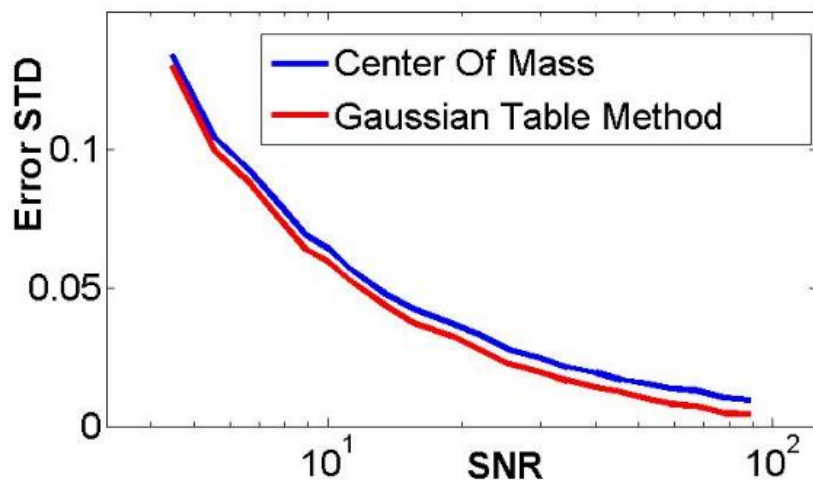

Fig. 2. Accuracy of determining the center of a single star for the center of mass method and the PDF table method
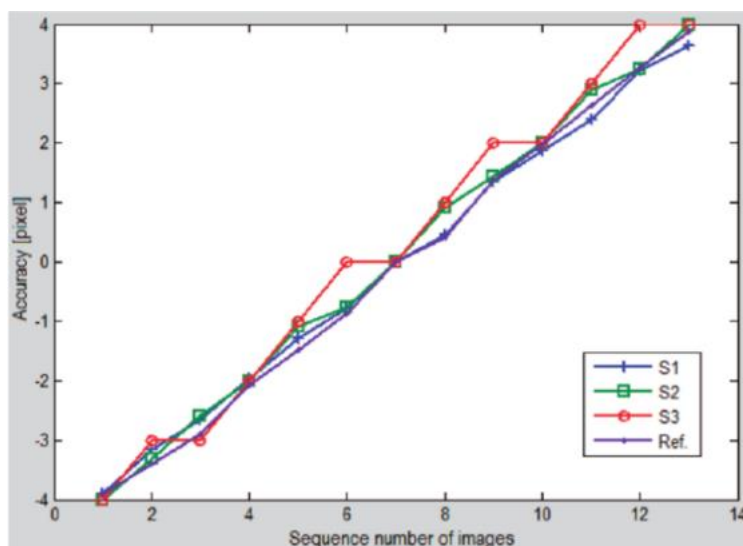

Fig. 3. Accuracy of centroid determination for the center of mass method

As follows from Fig. 3, the method demonstrates better accuracy, but has large errors for dim stars. The best results are obtained by the PSF fitting method. Determining the PSF fitting function at the beginning of image acquisition leads to an accurate calculation of the position of the stars in the entire series of analyzed images (fig. 4).

PSF-fitting can be used to calculate the centroids of stars on real images of the sky.

The orientation error of many modern star coaches is determined by systematic errors. Let's consider the influence of random and systematic sensor errors on the orientation accuracy of star trainers. The results of modeling the

main systematic errors due to underestimation of the inhomogeneity of the dark current are shown in fig. 5.
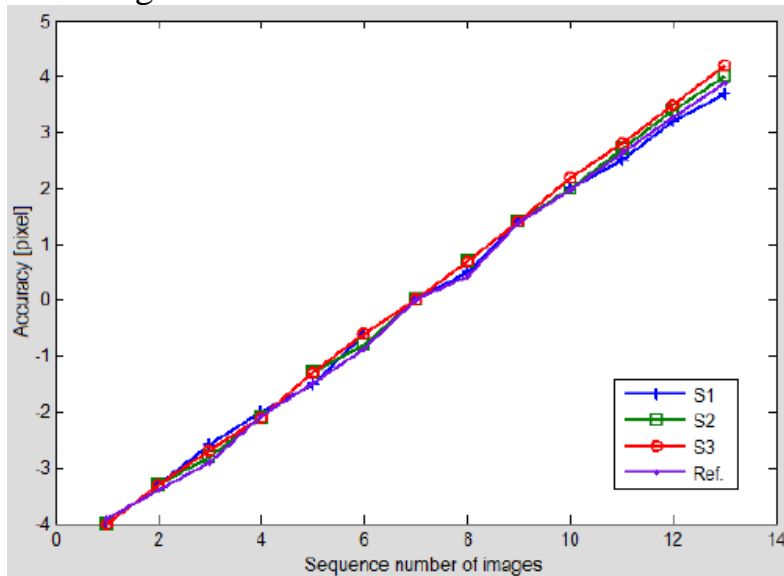

Fig. 4. Accuracy of centroid determination for the PSF fitting method. Results for three different stars S1, S2, S3 and reference calculation
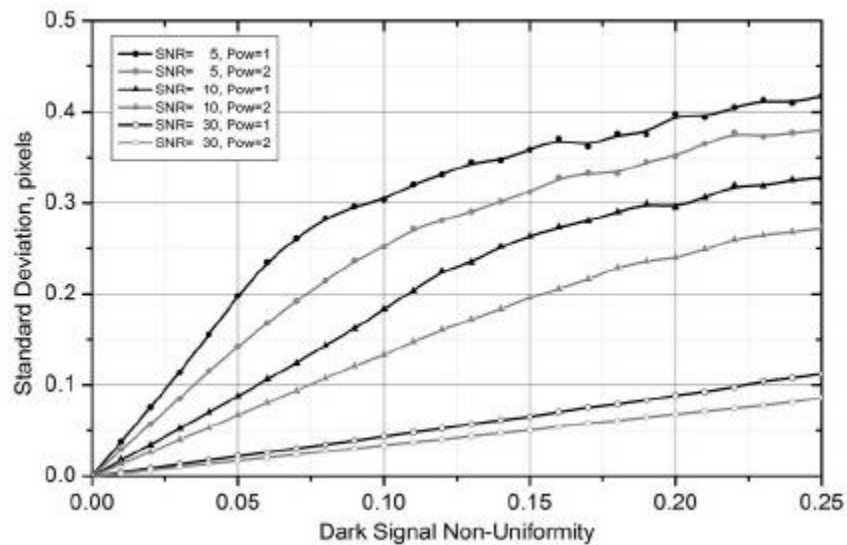

Fig. 5. Influence of the dark current inhomogeneity on the position determination error

The coordinate determination error caused by the inhomogeneity of the dark current at high signal levels is directly proportional to the value of the dark signal unevenness (DSNU) (the two lower curves in Fig. 5). At low signal levels SNR = 3 (signal/noise) and high DSNU values, this dependence differs from linear. This is due to the fact that with a large inhomogeneity of the dark current, the probability of detecting a star image decreases. Figure 5 shows the dependence of the error in the position of the photo centers on the DSNU value. Here

DSNU is the ratio of the standard deviation of the dark current to the average value. The curves are shown for three signal levels, which, in the absence of dark current inhomogeneity, give a signal-to-noise–SNR ratio.
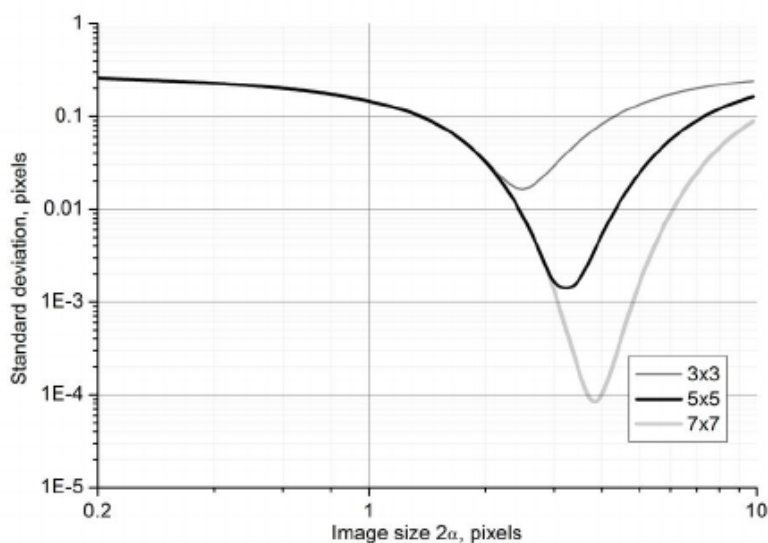

Fig. 6. Coordinate shift for images of small stars

Figure 6 shows the probability of detecting an image of a star depending on the unevenness of the dark current.

Figure 7 shows location errors associated with different true star locations (centroids). The coordinates of the center of gravity x and y changed in increments of 0,01 in the interval [-0,5: 0,5]. The SNR value is set by changing the noise level and leaving the brightness of the star constant. The PSF table method is more accurate, especially at high SNR.
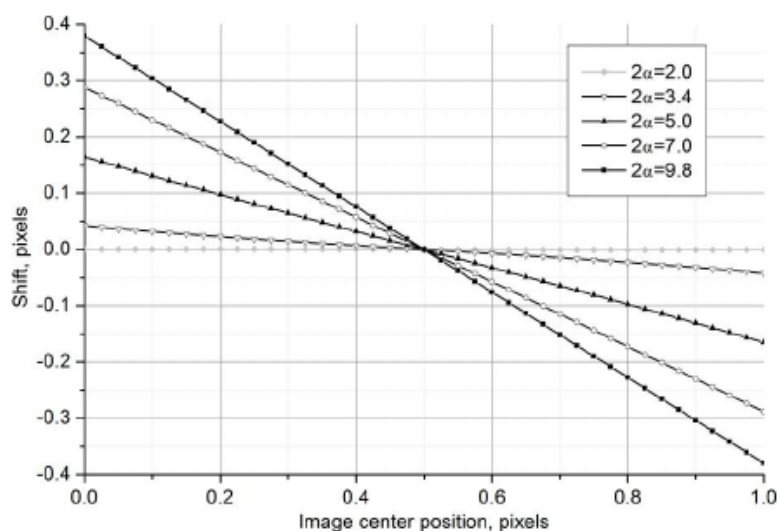

Fig. 7. Coordinate shift for images of large stars

The PSF function can be determined numerically based on the analysis of registered images. It detects image distortions as a result of atmospheric condi-

tions and parameters of recording equipment for a particular observation session and can be used to perform processing of subsequent images.
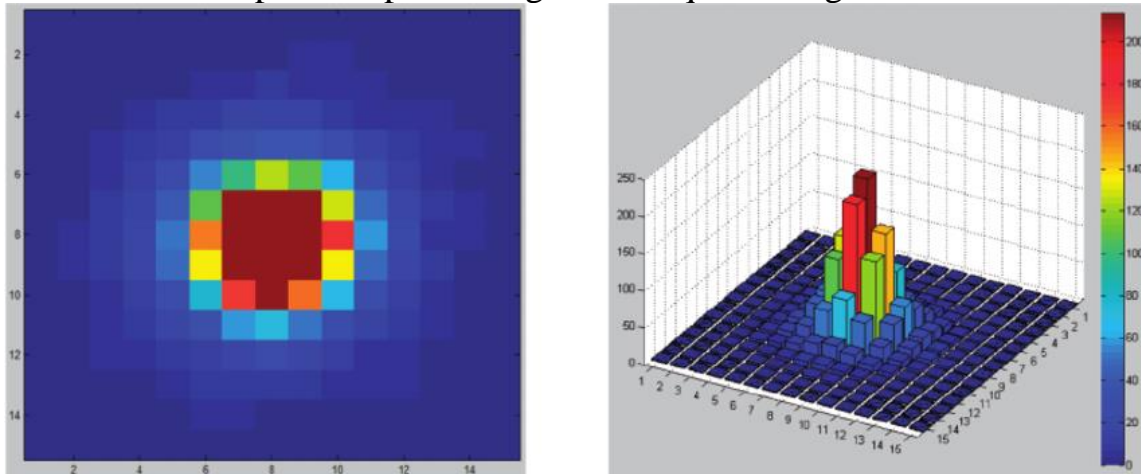

Fig. 8. Images of the sky: a) Star S2; b) contour of a bright star

The method of increasing accuracy allows using the PSF-fitting method to determine the position of stars in subsequent recorded images. The test image is executed several times, and the averaged PSF for several stars is calculated as a function of the template. Calculations of the averaged PSF take a lot of time, but they are performed once at the beginning of the observation session. The results of testing the test image algorithm in MATLAB for real images of the deep sky are shown in fig. 8.

When calculating the centroid, various optical effects can be taken into account, for example, distortion in the extreme areas of the image. As a result, the accuracy of the device will be increased. After recognition of stars and determination of the actual angular distances between them using previously prepared calibration functions, their identification is performed by comparing the obtained configurations with the configurations presented in the star catalog.

The histogram of the number of stars for the camera FOV 20 * × 15* is shown in fig. 9.
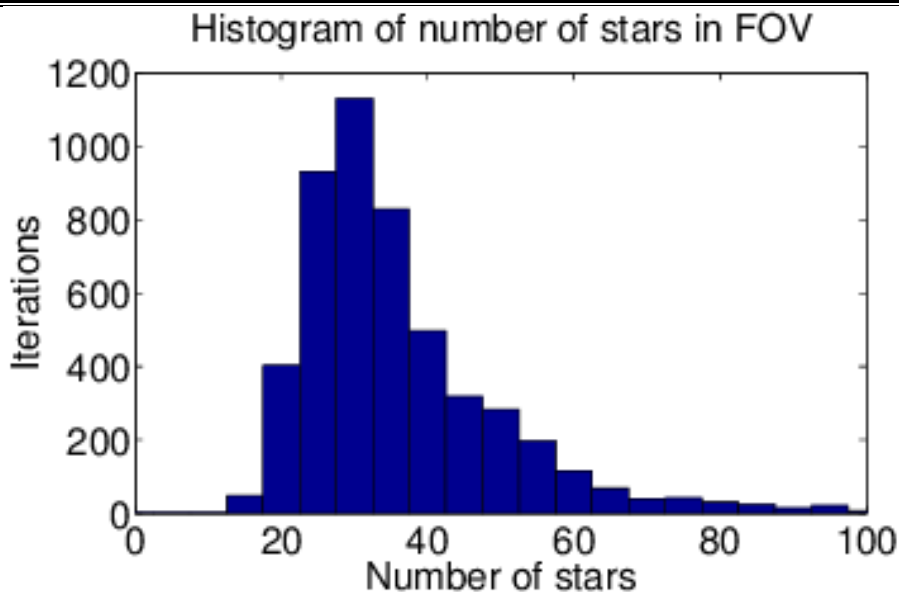
Fig. 9. Histogram of the number of stars

FOV cameras are used for image modeling. There are starless regions in the narrow FOV configuration. Therefore, a camera with a narrow focal length can only work in predefined areas.

The algorithm for determining the observed stars uses the 5 brightest objects in the image. One object is selected, angular distances to the remaining four are calculated, for each of which suitable pairs are found according to the list of distances. Next, a list of 5 stars is formed, for which the distance from the first to the other four is in the range $\delta \pm \varepsilon$, where ε is the accuracy of the sensor to determine the angular distance.

If there are "phantoms" (objects that are not present in the catalog) among the 5 selected stars in the image, then there will not be a single correct configuration in the list. In this case, the procedure for identifying stars is repeated with another set of stars.

The considered testing of the estimation of the position of the center of the star for slowly rotating satellites. In the case of a rapidly rotating satellite, the image is blurred, and the star shapes are stretched into long ellipses.

The fast tracking algorithm evaluates the position for subsequent images. A priori information about the current orientation of the camera and its angular velocity transmitted from the simulator to the frame processing module, prediction of the position of the corresponding stars in the detector coordinate system, recognition of selected image areas to confirm their presence can significantly increase the speed of the system as a whole.

Conclusions

A new method of filtering image distortions has been developed to improve the accuracy of determining the position of a star (centroid), consisting in using the method. Unlike other methods, for example, the center of mass meth-

od, it allows you to accurately calculate the positions of stars in the entire series of images of the starry sky.

Testing the algorithm of the method on model and real images confirmed an increase in the accuracy of determining orientation, and the package used for modeling determines the calculation time, the required memory, the size of the star catalog, and the sky coverage.

The algorithm can be optimized for specific camera configurations, which will further increase the accuracy of angular orientation measurement.

References

1. *Дятлов С. А.*, *Бессонов Р. В.* Обзор звездных датчиков ориентации космических аппаратов // Всероссийская научно-техническая конференция «Современные проблемы определения ориентации и навигации космических аппаратов» сборник трудов.-Россия.–2009.–С.: 12 – 31, https://elibrary.ru/contents.asp?id=33699680.

2. *Аванесов Г. А.*, *Бессонов Р. В.*, *Куркина А. Н.* Исследование погрешностей звездного датчика на основе данных летного эксперимента // Шестая Всероссийская научно-техническая конференция «Современные проблемы ориентации и навигации космических аппаратов», Россия, Таруса, 2018. – С.: 8 http://ofo.ikiweb.ru/publ/conf_2018_tez.pdf.

3. *Аванесов Г. А.* Исследование погрешностей звездных датчиков, вызванных термоупругими деформациями/ Г. А. Аванесов, Р. В. Бессонов, А. С. Квашнин, В. Е. Шевелев // Шестая Всероссийская научно-техническая конференция «Современные проблемы ориентации и навигации космических аппаратов», Россия, Таруса, 2018. – С.: 29 http://ofo.ikiweb.ru/publ/conf_2018_tez.pdf.

4. *Брысин Н. Н.* Исследование звёздных датчиков на электромагнитную совместимость/Н. Н. Брысин., К. П. Любченко, В. М. Муравьев, С. Н. Ромашин и др.// Шестая Всероссийская научно-техническая конференция «Современные проблемы ориентации и навигации космических аппаратов», Россия, Таруса. – 2018. – С.: 283 http://ofo.ikiweb.ru/publ/conf_2018_tez.pdf

5. *Малышев А. В.*, *Сазанов Г. С.* Идентификация параметров модели погрешности инерциальной навигационной системы разгонного блока посредством звездных датчиков // Материалы XXII конференции молодых ученых «Навигация и управление движением», Санкт-Петербург, 2020. – С.: 13-15, https://elibrary.ru/item.asp?id=44618751&selid=44618765

6. *Арефинкин А. А.* Методы повышения точности системы ориентации с контуром астрокоррекции малого космического аппарата дистанционного зондирования земли/ А. А. Арефинкин, В. В. Виленский, С. В. Воронков, С. Э. Зайцев и др.// Шестая Всероссийская научно-

техническая конференция «Современные проблемы ориентации и навигации космических аппаратов», Россия, Таруса. – 2018. – С.: 9 http://ofo.ikiweb.ru/publ/conf_2018_tez.pdf

7. *Аванесов Г. А.*, *Бессонов Р. В.*, *Куркина А. Н.* Технология наземной обработки данных о координатах звезд в целях повышения точности геопривязки снимков земли из космоса // Современные проблемы дистанционного зондирования Земли из космоса. Россия. – 2018. Т. 15. № 6. С. 31–38. http://jr.rse.cosmos.ru/article.aspx?id=2452

8. *Славгородский Д. А.* Погрешности гиростабилизированной системы оптического наблюдения, обусловленные особенностями кинематики оптического элемента // Материалы XXII конференции молодых ученых с международным участием. Санкт-Петербург. – 2020. – С.: 16-18, https://elibrary.ru/item.asp?id=44618751&selid=44618765

9. *Федорович С. Н.* Повышение точности изготовления роторов шаровых гироскопов методами прецизионной сфероводки // Материалы XXII конференции молодых ученых «Навигация и управление движением», Санкт-Петербург. 2020 – С.: 74. https://elibrary.ru/item.asp?id=44618751&selid=44618765

10. *Moldabekov M.* Proceedings of the SPIE/ M. Moldabekov, D. Akhmedov, S. Yelubayev, V. Ten, T. Bopeyev, K. Alipbayev, A. Sukhenko // The International Society for Optical Engineering, Amsterdam. – 2014, https://www.spiedigitallibrary.org/conference-proceedings-of-spie/9241/924122/Features-of-design-and-development-of-the-optical-head-of/10.1117/12.2067050.short

11. *Akhmedov D.* Proceedings of the SPIE/ D. Akhmedov, S. Yelubayev, V. Ten, T. Bopeyev, K. Alipbayev, A. Sukhenko // The International Society for Optical Engineering, Software and mathematical support of Kazakhstani star tracker. – 2016.

12. *Абубекеров М. К.* Способ повышения точности определения ориентации по звездам и длительного поддержания повышенной точности определения ориентации и устройство для их реализации/ М. К. Абубекеров, А. И. Захаров, М. Е. Прохоров, О. Ю. Стекольщиков // Интеллектуальная система тематического исследования наукометрических данных. Евразийский патент № 026970.– 30 июня 2017.

13. *Accardo D.*, *Rufino G.* Brightness-independent start-up routine for star trackers, IEEE Transactions on Aerospace and Electronics Systems. Vol. 38. № 3.–2002.– p. 813–823.